https://jksus.org

Journal of King Saud University – Science

2025 37 (3) 3412025

Research Article

Effect of 2,2'-bipyridine-4,4'-dicarboxylic acid-doped PVDF/KI/I2 based polymer electrolyte for dye sensitized solar cell applications

Sathya Krishnamoorthy[a], Kotteswaran Shanmugam[a,*], Jebapriya Mani[b], Gautham Devendrapandi[c], Ranjith Balu[d]

[a]Department of Chemistry, School of Basic Sciences, Vels Institute of Science Technology and Advanced Studies, Pallavaram, Chennai, 600117, Tamil Nadu, India
[b]Department of Chemistry, Mar Ephraem College of Engineering and Technology, Elavuvilai, Marthandam, 629171, Tamil Nadu, India
[c]Department of Computational Biology, Institute of Bioinformatics, Saveetha School of Engineering, Saveetha Institute of Medical and Technical Sciences, Thandalam, Chennai, 602105, Tamilnadu, India
[d]Division of Research and Development Cell, Lovely Professional University, Phagwara, Punjab, 144411, India

ARTICLE INFO

Keywords:
2,2'-Bipyridine-4,4'-dicarboxylic acid
Dye-sensitized solar cells
N, N-Dimethylformamide
Polymer electrolyte
Polyvinylidene fluoride

ABSTRACT

Solar energy transformation is a sustainable and dependable solution for rising energy demands and depleting fossil fuels. Dye-sensitized solar cells (DSSC) are one of the most popular solar energies conversions devices because of their simple fabrication, affordability, dependability, and high efficiency. Electrolytes are an essential component of DSSCs. They transfer electrons from the working electrode to the counter electrode and then return them to the photoanode via the polymer electrolyte. The performance of the 2,2'-Bipyridine-4,4'-dicarboxylic acid (2,2'-Bp-4,4'-dca)-doped Poly Vinylidene Fluoride (PVDF)/KI/I_2 polymer electrolyte was investigated to make an effective DSSC, using N, N-Dimethylformamide (DMF) as a solvent. The solution casting method were used to make 2,2'-Bp-4,4'-dca-doped PVDF/KI/I_2 electrolyte films with various weight percentages (0%, 10%, 20%, 30%, 40%, and 50%). The synthesized polymer electrolyte films were characterized using a variety of analyzing techniques including scanning electron microscopy (SEM), powdered X-ray diffractometer (PXRD), and AC-impedance analysis. PXRD studies verified that the strength of the peak gradually lowered up to 30% and then gradually increased. SEM analysis revealed that the size of spherical particles gradually decreased up to 30% of the 2,2'-Bp-4,4'-dca-doped PVDF/KI/I_2 polymer electrolyte. Ionic conductivity of the polymer electrolytes was calculated using AC-impedance analysis. The ionic conductivity of the 2,2'-Bp-4,4'-dca-undoped PVDF /KI /I_2 polymer electrolyte was 8.13×10^{-8} S cm^{-1}, this increased to 4.94×10^{-4} S cm^{-1} for the 30% 2,2'-Bp-4,4'-dca-doped PVDF/KI/I_2 electrolyte. It was proved to achieve the highest electrolytic conductivity compared with other weight percentages. The photovoltaic measurements were measured using fabricated DSSC. The maximum efficiency (η) (3.68%) was measured for 30% 2,2'-Bp-4,4'-dca-doped PVDF/KI/I_2. Therefore the 30% 2,2'-Bp-4,4'-dca-doped PVDF/KI/I_2 electrolyte was suitable for DSSC applications.

1. Introduction

The globe is currently experiencing a significant issue related to environmental pollution and a lack of safe, sustainable, and ecologically acceptable energy sources. The usage of non-renewable resources derived from mineral fuels, the shortage of power supplies, and the other elements linked with environmental and health problems like carbon dioxide emissions, air pollution, and greenhouse effects gives rise to several concerns (Ang *et al.* 2022; Østergaard *et al.* 2022; Sayed *et al.* 2023). As a result, there are efforts to reduce energy use investigate alternate energy sources to save the environment. Energy derived from resources that can be continuously renewed including sunlight, water, waves, rain, wind, and geothermal heat are typically called sustainable energy (Chand *et al.* 2022; Kumar *et al.* 2023). An endless supply of energy is expected to be available to people via non-exhaustive sources such as photoelectric cells, which use solar radiation to generate electricity. Given these issues, solar energy is among the most promising energy sources in the future because of its abundance, safety, cleanliness, and increased economic worth, all of which enable the production of electricity (Nastasi *et al.* 2022; Algarini *et al.* 2023). According to the estimation made by the European Joint Research Centre, energy consumption from solar energy in 2050 will account for 20% of overall energy consumption. By 2100, this percentage might cross 50% (Kant *et al.* 2022).

The photovoltaic cells may produce electricity without the need for moving parts or mechanical action (Solak *et al.* 2023). Depending on their manufacturing processes, materials, and operating principles, photovoltaic cells can be classified into several groups (Sampaio *et al.* 2022). The most widely utilized photovoltaic cell types include perovskite solar cells (Lee *et al.* 2022), silicon-cadmium telluride (Chowdhury *et al.* 2023), copper indium selenide/sulphide (Meng *et al.* 2022; Starzak *et al.* 2024), multiple-junction-based materials, and Dye-Sensitized Solar Cells (DSSC) (Febre *et al.* 2023). Earlier the photovoltaic cells were constructed with semiconductor-grade silicon and swiftly

***Corresponding author**
E-mail address: kotties555@gmail.com (Kotteswaran Shanmugam)

Received: 11 February, 2025 **Accepted:** 27 May, 2025 **Epub Ahead of Print:** 11 July, 2025 **Published:** 21 July, 2025

DOI: 10.25259/JKSUS_341_2025

emerged as the preferred power source for use on satellites. The usual solar power transformation efficiencies were very low (Pirdaus *et al.* 2023). However, barriers to their wider acceptance include the high cost of silicon cells and the usage of hazardous chemicals during their manufacturing. These elements lead researchers to hunt for less expensive, environmentally friendly solar cell substitutes (Agarwal *et al.* 2022). To rectify this the DSSCs have been used in practical applications, their conversion efficiency still needs to be raised. DSSCs use organic dyestuff molecules as a monolayer light absorber at the top of a mesoporous network of large band gap semiconductors known as nanocrystalline TiO_2. The concept of DSSCs was expanded by the realization of wet-type photocurrent generated devices which, was made possible by the interest in the photo electrochemistry of semiconductors (Zhou *et al.* 2022; Abdel-wahab *et al.* 2023). The polymer electrolyte used in DSSCs overcomes the problems caused by liquid electrolytes. These problems include shape flexibility, electrochemical stability, leakage, and sealing. Additionally, the presence of liquid electrolytes made it challenging to integrate large-area portions to implement combination structures and stop the attached dyes from desorbing and photodegrading in DSSCs (Mahalingam *et al.* 2023; Venkatesan *et al.* 2023). It also corroded the counter electrode and photodegraded certain components, which reduces the performance of the solar cells. The polymer electrolyte offers substitute materials for use in DSSC devices as a solution to this issue.

The four parts of the DSSC are as follows: Fluorinated tin oxide plate coated with nanocrystalline TiO_2 (Kotteswaran *et al.* 2018), which functions as an indicator electrode and absorbs the dye molecules. The electrolyte contains a redox pair (I^- / I^{3-}), which functions as a carrier of charges, quickly regenerating the oxidized dye molecule. Fluorinated tin oxide glass-plate coated with platinum functions as a counter electrode, regenerating the electrolyte. In DSSCs, the electrolytes are an essential component, which act as charge carriers between the electrodes during operation and renew the dye molecules. Many studies based on polymer electrolytes have been conducted in DSSCs to address the shortcomings of liquid electrolytes. DSSC have been made up of Pt as the photocathode, KI and I_2 in DMF as an oxidation-reduction pair (I- / I_3^-), and nanocrystalline TiO_2 with monolayer of photosensitizing dye (N719 dye) acting as a photoanode (Kotteswaran *et al.* 2021). For DSSC applications, many researchers have frequently employed alkali salts like potassium or lithium dissolved in polymers with high molecular weights such as polyvinylchloride, polyacrylonitrile, polyethylene oxide, poly vinylidene fluoride (PVDF), polymethylmethacrylate, etc., to generate polymer electrolyte systems (Dayanithi Janet *et al.* 2024). Many attempts have been made to decrease polymer crystallinity and increase ionic conductivity. To improve the DSSC performance many copolymerization and blending techniques have been introduced so far (Bhojanaa *et al.* 2022).

The PVDF polymer mixed with potassium iodide salts indicates that the combination process offers excellent electrical conductivity and boosts conversion efficiency for solar energy. Highly electronegative fluorine atom presents in PVDF, which have high molecular weight, contribute to enhancing the ionic conductivity of DSSCs (Kannadasan *et al.* 2018; Fachrirakarsie *et al.* 2024). Nitrogen containing organic groups present in the dopant also increase the charge transfer. The doped polymer electrolytes donate a pair of electrons that minimize iodine sublimation by working with iodine in the redox pair. The PVDF polymer garnered a lot of attention due to the -C-F functional group, which has strong electron withdrawing ability and crystalline phase (-VDF), as well as its elevated dielectric constant, which permits an elevated charge carrier concentration (Su'ait *et al.* 2023; Sasikumar Ragu *et al.* 2024). PVDF also has a strong -C-F functional group that withdraws electrons, which contributes to its electrochemical stability (Saud Premsingh *et al.* 2024; Zakaria *et al.* 2023). To improve the ionic conductivity of the polymer electrolytes a variety of techniques have been employed including the mixing of two polymers, the addition of organic dopants, and the utilization of nanofillers. Adding an organic dopant such as a nitrogenous organic molecule to the polymer electrolytes is the most effective technique (Wang *et al.* 2025). This may be the result of the polymer being mixed with an organic dopant, which can dramatically reduce the amount of crystallinity and increase the polymer electrolytes ionic conductivity, improving both the stability and efficiency of DSSC (Kusumavathi nita *et al.* 2023).

The heterocyclic organic compound contains nitrogen as a dopant, which interacts with the I^- /I^{3-} redox pair. The existence of the nitrogen atom's lone pair of electrons boosts the open circuit voltage (V_{oc}) and short circuit current (J_{sc}). The solid-state DSSC employing a 2,2'-Bp-4,4'-dca-doped with PVDF /KI /I_2 polymer electrolyte was reported in this work, which resulted in improved power conversion efficiency over an undoped PVDF/KI/I_2 polymer electrolyte (Bashir Shahid *et al.* 2022; Devadiga *et al.* 2022). It is anticipated that the presence of aromatic groups and carbon-nitrogen linkage will enhance the effectiveness of polymer electrolytes (Dissanayake *et al.* 2023; Habib *et al.* 2024; Zakiyah *et al.* 2024).

In this present work, various weight percentages of 2,2'-Bp-4,4'-dca-doped PVDF/KI/I_2 electrolyte films were made by a solution casting process using DMF as a solvent. Different weight percentages of 2,2'-Bp-4,4'-dca-doped PVDF/KI/I_2 polymer electrolyte were examined by powdered X-ray diffractometer (PXRD), scanning electron microscopy (SEM), and AC-Impedance analysis. The solar cell efficiency of the fabricated DSSC was investigated by photovoltaic measurements.

2. Materials and Methods

2.1 Materials

Polyvinylidene Fluoride with average M_w ~534,000 g/mol, glass plate coated with FTO (fluorine-doped tin oxide), 2,2'-Bipyridine-4,4'-dicarboxylic acid, Chloroplatinic acid hydrate, Titanium Tetrachloride, 4-tert-butanol, and Acetone was purchased from Sigma Aldrich. N, N-Dimethylformamide (DMF), Triton-X 100, Potassium Iodide (KI), Iodine (I_2), Ethanol (EtOH), Acetyl acetone, Acetonitrile (ACN) was purchased from Sisco Research Laboratories private limited, India. Titanium Dioxide, N719 Dye and Iodolyte were purchased from Solaronix`, SA. No additional purification was done for the above-mentioned chemicals.

2.2 Synthesis of polymer electrolyte

Solid state polymer electrolytes were produced using solution casting methodology (Sundaramoorthy *et al.* 2020). KI (0.03 g), PVDF (0.3 g), and I_2 (0.006 g) were first disintegrated in 20 mL of DMF solvent. The PVDF /KI /I_2 polymer electrolyte was synthesized by varying weight percentage (0%, 10%, 20%, 30%, 40%, and 50%) of 2,2'-Bp-4,4'-dca (with respect to KI) doped with polymer electrolytic solution. A homogenous polymer electrolytic solution was created by stirring the solution using an electromagnetic stirrer at 80°C for 12 h.

The homogeneous polymer solution was transferred into glass Petri dish to dry the polymer electrolyte solution. The solvent evaporated at 60°C in vacuum oven for 12 h. The schematic diagram of preparation of solid polymer electrolyte has been shown in Fig. 1. Various weight percentages (0%, 10%, 20%, 30%, 40%, and 50%) of 2,2'-Bp-4,4'-dca-doped PVDF/KI/I_2 polymer electrolytes were prepared for further characterizations.

2.3 Characterization of polymer electrolyte

Polymer electrolyte was characterized as follows. The PXRD analysis of various percentages of 0%, 10%, 20%, 30%, 40%, and 50% 2,2'-Bp-4,4'-dca-doped PVDF / KI / I_2 polymer electrolytes was obtained using Cu-Kα radiation in the range of 10-80° and a Bruker-advance D8 X-ray diffraction meter. The polymer electrolyte's surface morphology was examined by SEM analysis. An electrochemical workstation (Ametek, V3-500) was used to perform the AC-impedance. The bulk resistivity of the polymer electrolyte was measured using the Electrochemical Impedance Spectroscopy (EIS). Under 100 mW/cm^2 of light, the current-voltage curves of various percentages of 2,2'-Bp-4,4'-dca-doped polymer electrolyte based DSSCs have been measured.

2.4 Fabrication of DSSC

The various weight percentages of 2,2'-Bp-4,4'-dca doped PVDF/KI/I_2 polymer electrolyte were used between the working and counter electrodes of fabricated DSSC. The glass plate made of FTO were cleaned

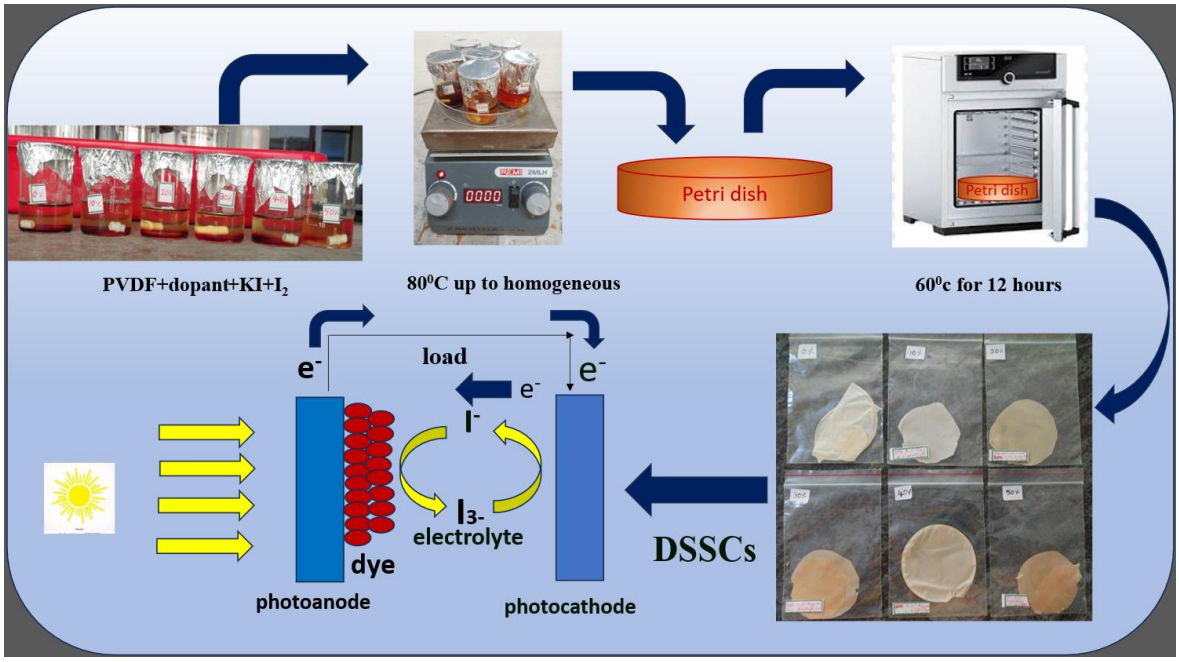

Fig. 1. Graphical representation of preparation of 2,2'-Bp-4,4'-dca doped PVDF/KI/I_2 polymer electrolyte.

with distilled water, ethanol, and acetone, using an ultrasonic bath for 30 min each. The TiO_2 colloidal paste was made by mixing 0.5 g of TiO_2 powder with a few drops of Triton X 100 and acetylacetone. FTO plates (0.5x0.5 cm^2) were fixed with cellulose tape, and then the TiO_2 paste was coated on the FTO plate using the "doctor blade" method. The FTO glass plates were sintered at 450°C for 3 h. The TiO_2-coated films were treated with $TiCl_4$ and sintered for 30 min at 450°C. Following that, the TiO_2-coated glass plates were immersed for 24 h in a 0.5 × 10^{-3} M N719 (photo-sensitizer) dye that contained 4-tertiary butanol and acetonitrile in a 1:1 volume ratio. To get rid of the unabsorbable dye, the TiO_2-coated glass plates were cleaned with ethanol and allowed to dry for 30 min. The drying temperature of the electrodes influences solvent evaporation, better dye adsorption, and good peel resistance. Inadequate or excessive drying temperatures can lead to peel-off issues or cracks, negatively affecting the device's ionic conductivity and efficiency. The electrode-coated area of the FTO glass plate was maintained at 0.5x0.5 cm^2 for DSSC fabrication. Chloroplatinic acid was coated on the FTO glass plate to prepare the cathode as the counter electrode. The FTO plates were sintered at 450°C for 3 h. The electron transport mechanism of DSSC has been shown in Fig. 2.

The detailed working principle of DSSC can be explained by the following eqs. (1)-(6):

(adsorbed by TiO_2) S + hv → (adsorbed by TiO_2) S* (1)

(adsorbed by TiO_2) S* → (adsorbed by TiO_2) S*+ (injected) e^- (2)

(adsorbed by TiO_2) S* + 3/2 I^- → (adsorbed by TiO_2) S* + ½ I^{3-} (3)

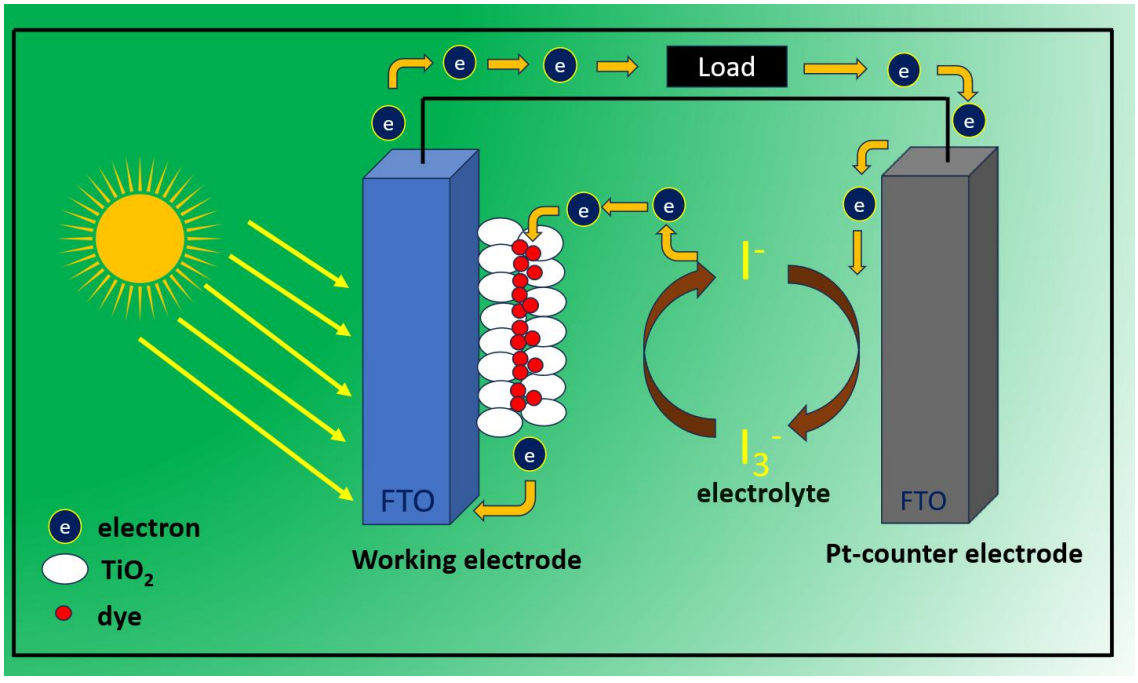

Fig. 2. Schematic representation of the electron transport mechanism of DSSC.

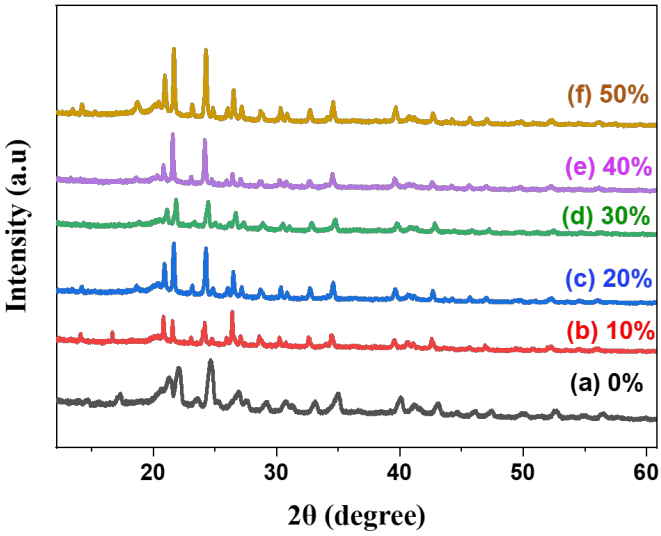

Fig. 3. PXRD patterns of 2,2'-Bipyridine-4,4'-dicarboxylic acid (a) 0%, (b) 10%, (c) 20%, (d) 30%, (e) 40% and (f) 50% doped PVDF/KI/I_2 electrolytic films.

$$I^{3-} + 2e^- \text{ (photo cathode)} \rightarrow 3\, I^- \text{ (photo cathode)} \quad (4)$$

$$\text{(adsorbed by } TiO_2) S^+ + e^- (TiO_2) \rightarrow \text{(adsorbed by } TiO_2) S \quad (5)$$

$$I^{-3} + 2e^- (TiO_2) \rightarrow 3I^- \text{ (photo anode)} \quad (6)$$

A photo-sensitizer absorbs the incident light (photon), which causes electrons in the dye to move from their ground state (s) to their excited state (S*). Now, excited electrons with a nanosecond lifetime are injected into the nanopore TiO_2 conduction band of the electrode, which is located beneath the dye excited state, and where light is absorbed by the dye molecule. These injected electrons diffuse into the FTO glass plate and move to the counter electrode (Azizi *et al.* 2019). When the electrons arrive at the counter electrode through the external circuit, electrons are conveyed to the electrolyte. As a result, I^- becomes I^{3-} and the electron moves to the ground state of the dye molecule for regeneration of the dye molecule. The process will occur continuously as long as the light source shines on the photoanode of the DSSC.

3. Results and Discussion

3.1 PXRD analysis

The PXRD analysis was investigated for pure and doped 2,2'-Bp-4,4'-dca PVDF/KI/I_2 to assess the phase purity and crystallinity of the polymer electrolyte (Prabakaran *et al.*, 2018). Fig. 3(a-f) depicts the PXRD patterns of (a) 0%, (b) 10%, (c) 20%, (d) 30%, (e) 40%, and (f) 50% 2,2'-Bp-4,4'-dca doped PVDF/KI/I_2 electrolytic films. The 2,2'-Bp-4,4'-dca-doped PVDF/KI/I_2 polymer electrolyte showed several low-intensity peaks in addition to the standard scanning angles of 2θ = 20.86, 21.57, 24.72, 26.91, and 35.04. The XRD peaks indicate the crystalline nature of the polymer electrolyte. The diffracted peak intensities of 0%, 10%, 20%, and 30% of 2,2'-Bp-4,4'-dca-doped PVDF/KI/I_2 gradually reduced. For 40% and 50% doped polymer electrolyte, the intensity started to increase. It shows that the polymer electrolyte's crystallinity reduced from 0% to 30% dopant, and then increased for 40% and 50% additions of dopant.

When 2,2'-Bp-4,4'-dca was added to pure PVDF/KI/I_2 the polymer chain rearrangement was hindered, resulting in a distinctly disordered polymer structure. This analysis of the data depicted that the PVDF/KI/I_2 polymer doped with 30% 2,2'-Bp-4,4'-dca had the lowest crystallinity of solid polymer electrolyte, and it was more amorphous than other electrolytes. When the amorphous nature of the polymer electrolyte increased, the ionic conductivity of the polymer electrolyte also increased (Gunasekaran *et al.* 2020).

3.2 AC-Impedance analysis

The bulk resistance for the polymer electrolyte was measured using AC-impedance spectroscopy (Nadia *et al.* 2017). Fig. 4(a-f) displays the impedance graph for the various weight percentages of 2,2'-Bp-4,4'-dca-doped PVDF/KI/I_2 polymer electrolyte. Based on the AC-impedance spectroscopy, the following formula was used to measure the ionic conductivity (σ) of the polymer electrolyte film.

Ionic Conductivity (σ) = t /R_b*A.

"t" stands for the polymer electrolyte thickness, "A" stands for the polymer electrolyte layer, which covers the electrode area, and "Rb" stands for the bulk resistance of the polymeric electrolyte (Arof *et al.*

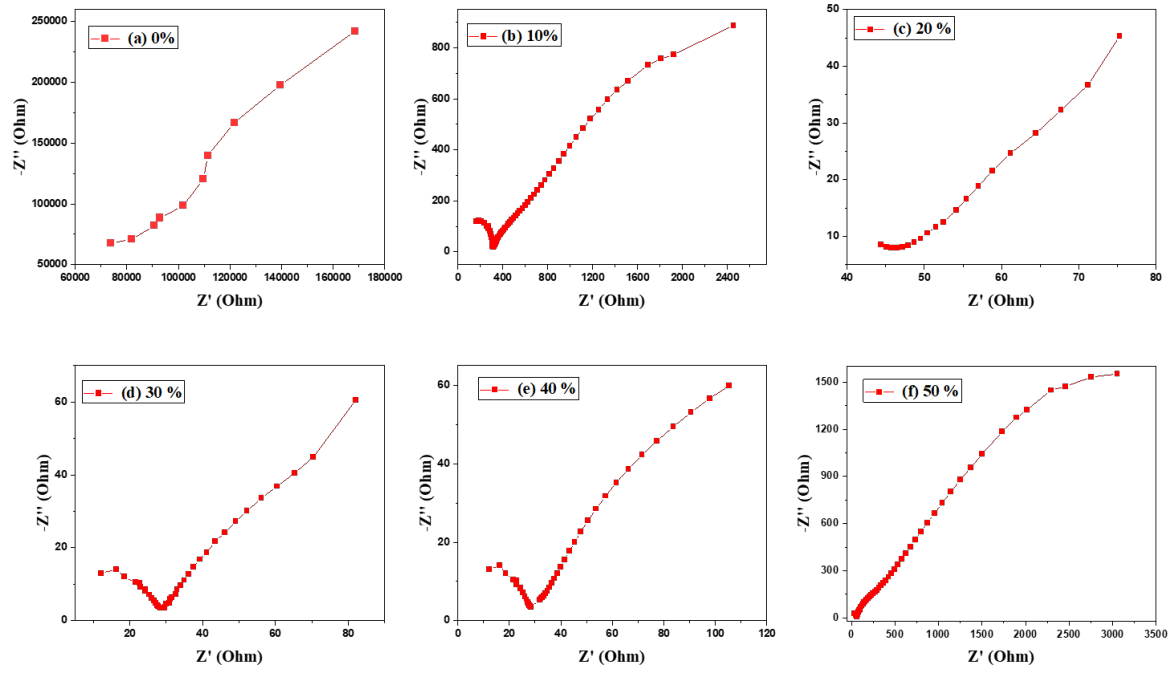

Fig. 4. AC-impedance analysis of 2,2'-Bp-4,4'-dca (a) 0%, (b) 10%, (c) 20%, (d) 30%, (e) 40% and (f) 50% doped PVDF/KI/I_2 electrolytic films.

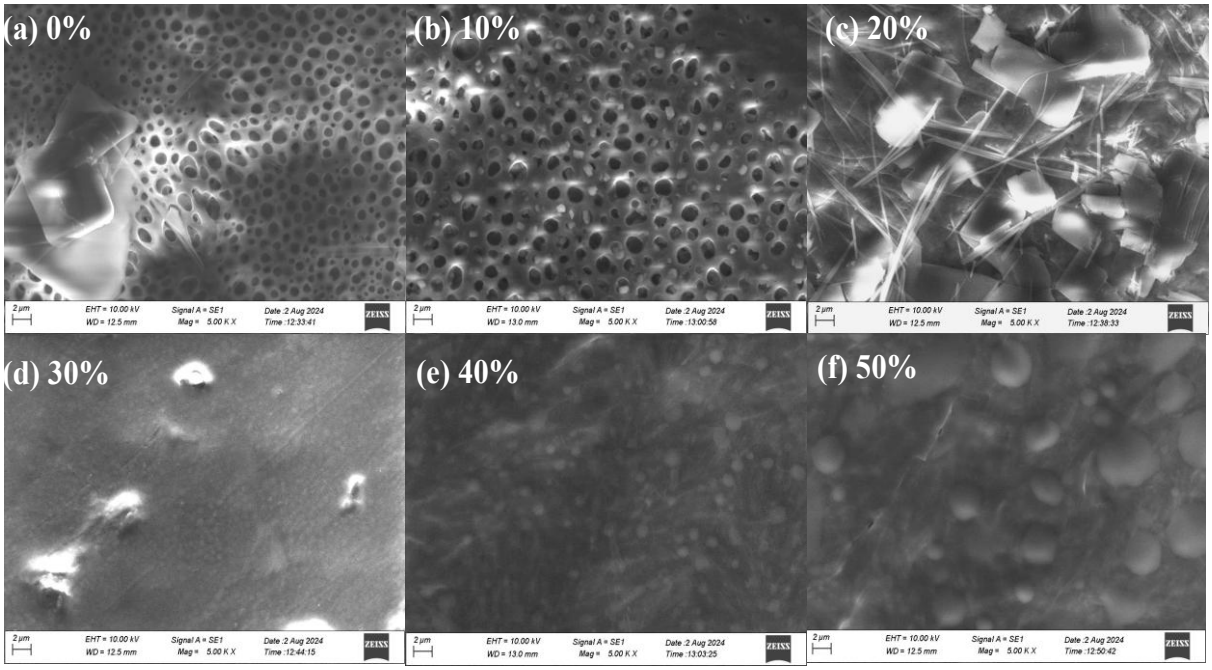

Fig. 5. SEM images of 2,2'-Bipyridine-4,4'-dicarboxylic acid (a) 0%, (b) 10%, (c) 20%, (d) 30%, (e) 40% and (f) 50% doped PVDF/KI/I_2 electrolyte films.

2017). The measured conductivity value of the undoped PVDF /KI /I_2 polymer electrolyte was 8.13 x 10^{-8} Scm^{-1}.

The ionic conductivities of 10%, 20%, 30%, 40%, and 50% doped polymer electrolyte were 3.68 x 10^{-5} Scm^{-1}, 1.20 x 10^{-5} Scm^{-1}, 4.94 x 10^{-4} Scm^{-1}, 4.28 x 10^{-4} Scm^{-1}, and 1.75 x 10^{-4} Scm^{-1}, respectively.

The effective interaction of the dopant with PVDF/KI/I_2 resulted in the highest conductivity. The maximum value of ionic conductivity 4.94 x 10^{-4} Scm^{-1} was observed at 30% of 2,2'-Bp-4,4'-dca-doped PVDF/KI/I_2 polymer electrolyte. The ionic conductivities of polymer electrolytes between 0% to 30% gradually increased, and further addition of dopant decreased the ionic conductivities. The nitrogen-containing organic compounds like 2,2'-Bp-4,4'-dca, when combined with redox couple (iodine and triiodide), created a charge-transfer complex, which lowered iodine sublimation, increased conductivity, and increased efficiency of the solar cell (Kesavan *et al.* 2018).

3.3 SEM analysis

The surface morphology of PVDF/KI/I_2 doped with various weight percentages of 2,2'-Bp-4,4'-dca was examined with SEM analysis. Fig. 5(a-f) illustrates the notable distinctions between pure PVDF/KI/I_2 and 2,2'-Bp-4,4'-dca-doped PVDF/KI/I_2 polymer electrolytes. The porosity and particle size of the polymer electrolytes were compared (Abisharini *et al.* 2020). The pore nature and particle size of the undoped and 10%, 20%, 40%, and 50% 2,2'-Bp-4,4'-dca-doped PVDF/KI/I_2 polymer electrolyte was larger than the 30% doped polymer electrolyte.

The 30% doped polymer electrolyte had a smooth surface, finer structure, and smaller particle size, indicating a more amorphous nature, which led to improvement in the ionic conductivity.

3.4 Photovoltaic performance

Every component of a DSSC has a significant impact on stability and efficiency. To start, improving light transmittance and electrical conductivity are qualities necessary for a glass substrate made of conducting oxide. Second, there is a large area occupied by reaction sites available for the incident absorption light due to the porosity, shape, and number of dye molecules absorbed on the TiO_2 surface. Third, additional electrolytes in solid states are used to counteract the volatilization issue associated with liquid electrolytes, such as iodine and triiodide, which are used as liquid electrolytes in redox mediators. Fig. 6(a-f) displays the current–voltage (J–V) curves for the DSSC made

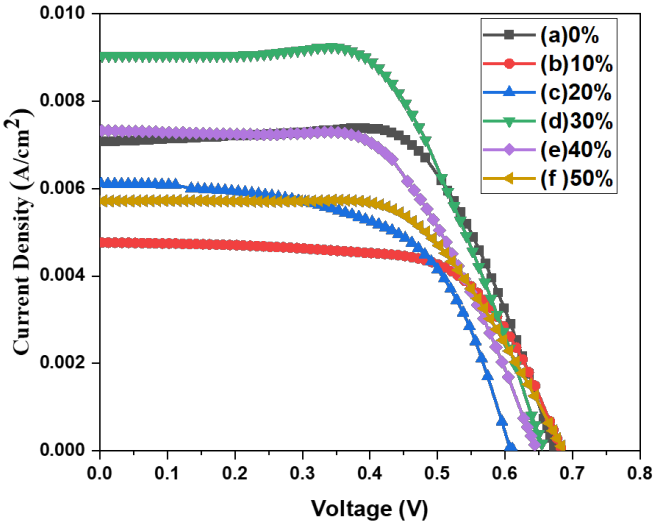

Fig. 6. The photovoltaic (J-V) curves for DSSCs of (a) 0%, (b) 10%, (c) 20%, (d) 30%, (e) 40% and (f) 50% 2,2'-Bipyridine-4,4'-dicarboxylic acid doped with PVDF / KI/I_2 electrolytes.

of 0%, 10%, 20%, 30%, 40%, and 50% 2,2'-Bp-4,4'-dca-doped with PVDF/KI/I_2 electrolytes. To measure the solar cell efficiency η (%) of solar cells, the following formula was used:

$$\eta\ (\%) = (V_{oc} \times J_{sc} \times FF / P_{in}) \times 100$$

where η denotes the power conversion efficiency (%) and **FF** represents the fill factor (%). $\mathbf{J_{sc}}$ denotes the short circuit current density (mA/cm^2) and $\mathbf{V_{oc}}$ represents the open circuit voltage (mV). The incident light power is $\mathbf{P_{in}}$. $\mathbf{J_{max}}$ (mA/cm^2) and $\mathbf{V_{max}}$ (mV) represent the voltage and current, respectively at the greatest power output in the J-V curve (Singh Rahul *et al.* 2017).

The photovoltaic parameters of fabricated DSSC with 2,2'-Bp-4,4'-dca (0%, 10%, 20%, 30%, 40%, and 50%)-doped PVDF /KI /I_2 electrolytes were exhibited. The pure PVDF/KI/I_2 based solar cell parameters were J_{sc}=4.16 mA/cm^2, V_{oc}=0.67 V, FF=59.13%, and η=1.64%. The 10% PVDF/KI/I_2 based solar cell parameters were J_{sc}=4.80 mA/cm^2,

Table 1.
The photo voltaic parameters of DSSCs of (a) 0%, (b) 10%, (c) 20%, (d) 30%, (e) 40%, and (f) 50% of 2,2'-Bipyridine-4,4'-dicarboxylic acid doped PVDF/ KI/I_2 electrolytes.

DSSC	2,2'-Bipyridine-4,4'-dicarboxylic acid (%)	J_{sc} (mA/cm^2)	V_{oc} (V)	FF (%)	η (%)
a	0	4.16	0.67	59.13	1.64
b	10	4.80	0.68	65.59	2.14
c	20	5.97	0.62	68.45	2.53
d	**30**	**9.04**	**0.66**	**61.81**	**3.68**
e	40	7.33	0.65	60.75	2.89
f	50	5.79	0.68	62.03	2.44

Significant values are highlighted in bold.

V_{oc}=0.68 V, FF= 65.59%, and η=2.14%. The 20% PVDF/KI/I_2 based solar cell parameters were J_{sc}=5.97 mA/cm^2, V_{oc}=0.62 V, FF=68.45%, and η=2.53%. The 30% PVDF/KI/I_2 based solar cell parameters were J_{sc}=9.04 mA/cm^2, V_{oc}=0.66 V, FF=61.81% and η=3.68%. The 40% PVDF/KI/I_2 based solar cell parameters were J_{sc}=7.33 mA/cm^2, V_{oc}=0.65 V, FF=60.75%, and η=2.89%. Lastly, the 50% PVDF/KI/I_2 based solar cell parameters were J_{sc}=5.79 mA/cm^2, V_{oc}=0.68 V, FF=62.03%, and η=2.44%. All these parameters have been listed in Table 1. Photovoltaic measurements indicate that 2,2'-Bp-4,4'-dca doped PVDF /KI /I_2 solar cell performed better than the undoped electrolyte. This could be attributed to the compounds maximum π-electron density as well as the presence of a lone pair of electrons present in -N atom (Moharam *et al.* 2021). Furthermore, 2,2'-Bp-4,4'-dca raises I^- concentration while lowering I_3^- ion concentration. As a result, there is less I_2 sublimation, which improves DSSC stability.

$$2,2'\text{-Bp-4,4'-dca} + I_3^- \rightarrow (2,2'\text{-Bp-4,4'-dca})\ I_2 + I^- \quad (7)$$

$$2(2,2'\text{-Bp-4,4'-dca}) + I_3^- \rightarrow (2,2'\text{-Bp-4,4'-dca})_2 I^+ + I^-. \quad (8)$$

The reaction between the injected electron and I_3^- may be reduced by the drop in I_3^- concentration at the electrolyte junction of semiconductors, which raises the concentration of electrons that enhances the cell V_{oc}. Simultaneously, an elevation in I^- concentration causes an increase in I^- hole collection, which raises the cells I_{sc}. Owing to their increased ionic conductivity and more amorphous nature, 2,2'-Bp-4,4'-dca-doped PVDF/KI/I_2 polymer electrolyte-based DSSCs with 30% concentration exhibited a higher photon-current conversion efficiency η =3.68%, with the measurements of J_{sc}=9.04 mA/cm^2, V_{oc}=0.66 V, FF=61.81%. When doping 0%, 10%, and 20% concentration of the dopant in the polymer electrolyte, it was low and did not sufficiently alter the charge transfer properties. When doping 40% and 50% dopant into the polymer electrolyte, it was high, and the dopant caused aggregation or ion clustering, which potentially hindered the ion movement and reduced conductivity. Therefore, 30% doping provides the best balance between low and enhanced ionic conductivity, resulting in higher efficiency. In this 30% doping, the aggregation and clustering decreases and the ion transport properties increases. So, 30% of dopant gives the enhanced ionic conductivity and high solar cell efficiency.

These results show that the 30% 2,2'-Bp-4,4'-dca-doped PVDF/ KI / I_2 electrolyte performs better than the 0%, 10%, 20%, 40%, and 50% doped 2,2'-Bp-4,4'-dca PVDF/ KI / I_2 electrolyte in DSSCs. From 0% doped polymer electrolyte, the parameters of fill factor, open circuit voltage, and short circuit current density gradually increased up to 30% and attained the maximum power conversion efficiency (η) at 3.68%. While increasing the incorporation of dopant into the polymeric electrolyte, the fill factor, open circuit voltage, and short circuit current density started to decrease with decreasing the power conversion efficiency (η). Numerous reports had stated that adding additives, including nitrogen heterocyclic compound might raise the anode's conducting band and raise the V_{oc}. The solvent has been an important medium that allows the redox reaction to occur by dissolving the additive and the redox pair. Fig. 7 exhibits the best composition of power transformation efficiency of DSSCs using 2,2'-Bp-4,4'-dca doped with PVDF / KI / I_2 electrolytes.

The molecular interaction of 2,2'-Bp-4,4'-dca doped PVDF / KI / I_2 electrolyte have been expressed in Fig. 8. The nitrogen atoms in the pyridine rings can act as electron donors, and the carboxylic acid groups can act as donors of protons. The mechanical strength and ionic conductivity of the solid polymeric electrolyte must be balanced. Ionic species are generally distributed throughout the polymer matrix, which facilitates the moving of ions between the dye-coated photoanode and counter electrode. To ensure high efficiency and endurance of the DSSC, appropriate integration and interaction of these components are critical to the overall effectiveness of the solid polymer electrolyte. Thus, it can be concluded that the transformation efficiency of DSSC increased with the addition of 2,2'-Bp-4,4'-dca to PVDF/KI/I_2. The 30% 2,2'-Bp-4,4'-dca PVDF /KI /I_2 electrolytes were used to improve the device efficiency and ionic conductivity. The comparative study of reported solar cell efficiency of different dopants with polymer materials has been given in Table 2. It is clear that the donor of electrons qualities in the polymeric electrolyte of 2,2'-Bp-4,4'-dca had a notable impact on the DSSC performance.

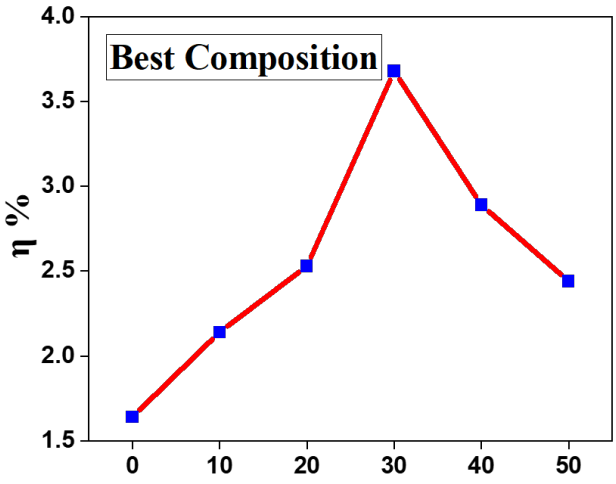

Fig. 7. Power transformation efficiency of DSSCs using 2,2'-Bipyridine-4,4'-dicarboxylic acid doped with PVDF / KI / I_2 electrolytes.

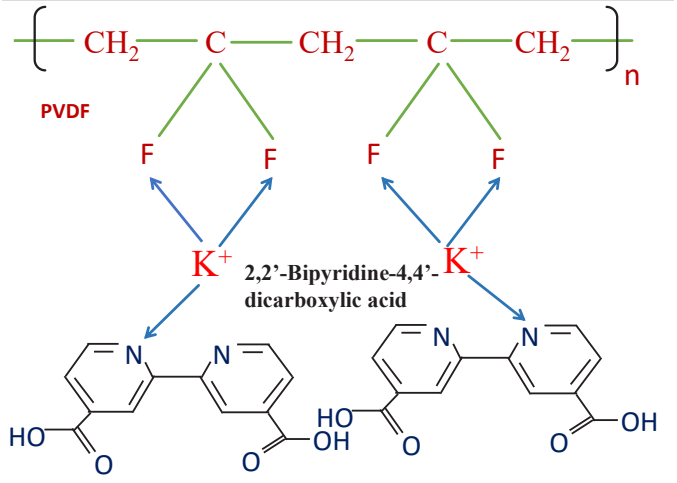

Fig. 8. Molecular interaction of 2,2'-Bipyridine-4,4'-dicarboxylic acid with PVDF / KI / I_2 electrolytes.

Table 2.
Solar cell efficiency comparison

S. No	Doped polymer electrolyte	Efficiency (%)	Year	Reference
1	propylene carbonate ethylene carbonate-doped PVDF matrix	1.79%	2015	Wang *et al.*,
2	4-nitroaniline-doped PVDF-HFP/LiI/I2	1.5%	2017	Kannadasan *et al*
3	Phenothiazine- doped PVDF-HFP/KI/I2	2.92%	2017	R A Senthil *et al*
4	2-Amino-4,6-Dimethoxypyrimidine-doped PVDF/KI/I2	2.5%	2020	Sundaramoorthy *et al*
5	30% 2,2'-Bipyridine-4,4'-dicarboxylic acid-doped PVDF/KI/I2	3.68%	2025	Present work

4. Conclusion

The present research work has been studied with 2,2'-Bp-4,4'-dca (0%, 10%, 20%, 30%, 40%, and 50%)-doped PVDF/KI/I_2 electrolytes using PXRD, AC-Impedance, and SEM analysis. According to the PXRD spectra, 30% 2,2'-Bp-4,4'-dca-doped PVDF/KI/I_2 polymer electrolyte exhibited a more amorphous nature. Furthermore, investigations on ionic conductivity showed that 30% 2,2'-Bp-4,4'-dca-doped PVDF/KI/I_2 electrolyte achieved the maximum ionic conductivity as 4.94 X 10^{-4} Scm^{-1}. The prepared polymer electrolyte's surface morphology was further clarified by SEM analysis, which shows that the 30% dopant has the smallest particles with a smooth and fine surface. DSSCs have been fabricated using various weight percentages of (from 0% to 50%) 2,2'-Bp-4,4'-dca doped PVDF/ KI/I_2 polymer electrolyte. The efficiency of 3.68%, the DSSC using the PVDF/KI/I_2 electrolyte doped with 30% 2,2'-Bp-4,4'-dca showed the highest performance. This shows that the performance of DSSCs is significantly impacted by the 2,2'-Bp-4,4'-dca doping concentration, with 30% doping producing the best results in this investigation.

CRediT authorship contribution statement

Sathya Krishnamoorthy: Conceptualization, Data Curation, Formal Analysis, Writing-original draft, **Kotteswaran Shanmugam:** Investigation, Visualization, writing-original draft, Methodology, Supervision, Wring-reviews and editing. **Jebapriya Mani:** Visualization, Writing-reviews & editing. **Gautham Devendrapandi:** Conceptualization, Data curation, Visualization, **Ranjith Balu:** Investigation, visualization, Software, Writing-original draft.

Declaration of competing interest

The authors declare that they have no known competing financial interests or personal relationships that could have appeared to influence the work reported in this paper.

Declaration of Generative AI and AI-assisted technologies in the writing process

The authors confirm that there was no use of artificial intelligence (AI)-assisted technology for assisting in the writing or editing of the manuscript and no images were manipulated using AI.

Reference

Abdel-Wahab, E. M. O. S., 2023. Novel Multi-Junction Solar Cell Structures Based on Silicon Substrates (Doctoral dissertation, Benha University).

Abisharani, J. M., DineshKumar, R., Devikala, S., Arthanareeswari, M., Ganesan, S., 2020. Influence of 2, 4-Diamino-6-Phenyl-1-3-5-triazine on bio synthesized TiO2 dye-sensitized solar cell fabricated using poly (ethylene glycol) polymer electrolyte. Materials Res Express 2, 025507. Doi :10.1088/2053-1591/ab7066

Agrawal, A., Siddiqui, S.A., Soni, A., Sharma, G.D., 2022. Advancements, frontiers and analysis of metal oxide semiconductor, dye, electrolyte and counter electrode of dye sensitized solar cell. Solar Energy 233, 378-407. https://doi.org/10.1016/j.solener.2022.01.027

Algarni, S., Tirth, V., Alqahtani, T., Alshehery, S. and Kshirsagar, P., 2023. Contribution of renewable energy sources to the environmental impacts and economic benefits for sustainable development. Sustainable energy technologies and assessments, 56, p.103098. https://doi.org/10.1016/j.seta.2023.103098

Ang, T.Z., Salem, M., Kamarol, M., Das, H.S., Nazari, M.A. and Prabaharan, N., 2022. A comprehensive study of renewable energy sources: Classifications, challenges and suggestions. Energy strategy reviews, 43, p.100939. https://doi.org/10.1016/j.esr.2022.100939

Arof, A.K., Noor, I.M., Buraidah, M.H., Bandara, T.M.W.J., Careem, M.A., Albinsson, I., Mellander, B.-E., 2017. Polyacrylonitrile gel polymer electrolyte-based dye sensitized solar cells for a prototype solar panel. Electrochimica Acta 251, 223-234. https://doi.org/10.1016/j.electacta.2017.08.129

Azizi, T., Toujeni, H., Karoui, M.B. and Gharbi, R., 2019, March. A comprehensive device modeling of solid-state dye sensitized solar cell with SCAPS-1D. In 2019 19th International Conference on Sciences and Techniques of Automatic Control and Computer Engineering (STA) (pp. 336-340). IEEE. https://doi.org/10.1109/STA.2019.8717282

Bashir, S., Iqbal, J., Farhana, K., Jafer, R., Hina, M., Kasi, R., Subramaniam, R.T. Hybrid organic polymer electrolytes for dye-sensitized solar cells. In: Dye-Sensitized Solar Cells Dye-Sensitized Solar Cells: Elsevier), pp. 181-212. https://doi.org/10.1016/b978-0-12-818206-2.00006-2

Bhojanaa, K.B., Kannadhasan, S., Santhosh, N., Vijayakumar, P., Senthil Pandian, M., Ramasamy, P., Pandikumar, A., 2020. Enhanced electrochemical and photovoltaic performance for MoO3 nanorods at different calcination temperature-based counter electrode in Pt-free dye-sensitized solar cells applications. SN Appl Sci 2. https://doi.org/10.1007/s42452-020-03555-8

Chand, A.A., Lal, P.P., Prasad, K.A. and Kumar, N.M., 2022. Economics and environmental impacts of solar energy technologies. In Solar Energy Advancements in Agriculture and Food Production Systems (pp. 391-423). Academic Press. https://doi.org/10.1016/b978-0-323-89866-9.00006-7

Chowdhury, T.A., Bin Zafar, M.A., Sajjad-Ul Islam, M., Shahinuzzaman, M., Islam, M.A., Khandaker, M.U., 2023. Stability of perovskite solar cells: Issues and prospects. RSC Adv. 13, 1787-1810. https://doi.org/10.1039/d2ra05903g

Dayanithi, J., Pichaikaran, S., Selvam, S., Kotteswaran, S., Kumaresan, N., Pugazhendhi, A., Rajesh Kumar, M., Al Garalleh, H., Ali Alshehri, M., Murugadoss, G., 2024. 4-Carboxyphenyl as efficient donor group in nano Zn-Porphyrin for dye sensitized solar cells. Environ Res 251, 118704. https://doi.org/10.1016/j.envres.2024.118704

Devadiga, D., Selvakumar, M., Devadiga, D., Ahipa, T.N., Shetty, P., Paramasivam, S. and Kumar, S.S., 2022. Synthesis and characterization of a new phenothiazine-based sensitizer/co-sensitizer for efficient dye-sensitized solar cell performance using a gel polymer electrolyte and Ni–TiO 2 as a photoanode. New Journal of Chemistry, 46(44), pp.21373-21385.https://doi.org/10.1039/D2NJ03589H

Dissanayake, M.A.K.L., Hettiarachchi, M.S.H., Senadeera, G.K.R., Kumari, J.M.K.W., Umair, K., Bandara, T.M.W.J., Albinsson, I., Furlani, M., Mellander, B.-E., Chaure, N.B., Olusola, O.I., 2023. High-efficiency dye-sensitized solar cells fabricated with electrospun PVdF-HFP polymer nanofibre-based gel electrolytes. Bull Mater Sci 46. https://doi.org/10.1007/s12034-023-02919-1

Fabre, B., Loget, G., 2023. Silicon photoelectrodes prepared by low-cost wet methods for solar photoelectrocatalysis. Acc Mater Res 4, 133-142. https://doi.org/10.1021/accountsmr.2c00180

Fachrirakarsie, F.F., Kusumawati, N., 2024. The effect of polyetherimide polymer membrane composition on the performance efficiency of dye sensitized solar cell (DSSC) based on natural photosensitizer of butterfly pea flowers. J Pijar MIPA 19, 507-513. https://doi.org/10.29303/jpm.v19i3.6636

Gunasekaran, A., Sorrentino, A., Asiri, A.M., Anandan, S., 2020. Guar gum-based polymer gel electrolyte for dye-sensitized solar cell applications. Solar Energy 208, 160-165. https://doi.org/10.1016/j.solener.2020.07.084

Habib, A., Metwally, M.M., Fahmy, T., 2024. Efficient single-crystal 4-N, N-dimethylamino-4-N-methyl-stilbazolium tosylate (DAST) on the optical, piezoelectric coefficient and structure of P (VDF-HFP) copolymer for energy conversion systems. Polymer Bulletin. 81, 6513-6537. https://doi.org/10.1007/s00289-023-05016-9

Kannadhasan, S., Pandian, M.S., Ramasamy, P., 2017. Synthesis of pure and 4-nitroaniline doped (PVDF-HFP/LiI/I2) polymer electrolyte for dye sensitized solar cell (DSSC) applications. Dae Solid State Physics Symposium 2016 Bhubaneswar, Odisha, India, pp. 050061. https://doi.org/10.1063/1.4980294

Kannadhasan, S., Pandian, M.S., Ramasamy, P., 2018. Synthesis of pure and benzoguanamine-doped PVDF/KI/I2 electrolytes for dye sensitized solar cell (DSSC) applications. Dae Solid State Physics Symposium 2017 Mumbai, India, pp. 140034. https://doi.org/10.1063/1.5029165

Kant, N., Singh, P., 2022. Review of next generation photovoltaic solar cell technology and comparative materialistic development. Materials Today: Proceedings 56, 3460-3470. https://doi.org/10.1016/j.matpr.2021.11.116

Kesavan, M., Arulraj, A., Rajendran, K., Anbarasu, P., Ganesh, P.A., Jeyakumar, D., Ramesh, M., 2018. Performance of dye-sensitized solar cells employing polymer gel as an electrolyte and the influence of nano-porous materials as fillers. Mater. Res. Express 5, 115305. https://doi.org/10.1088/2053-1591/aade2a

Kotteswaran, S., Pandian, M.S., Ramasamy, P., 2018. Synthesis, optical, electrochemical and photovoltaic properties of donor modified organic dyes for dye-sensitized solar cell (DSSC) applications. J Mater Sci: Mater Electron 29, 6672-6678. https://doi.org/10.1007/s10854-018-8653-8

Kotteswaran, S., Ramasamy, P., 2021. The influence of triphenylamine as a donor group on Zn–porphyrin for dye sensitized solar cell applications. New J Chem 45, 2453-2462. https://doi.org/10.1039/d0nj05060a

Kumar, C.M.S., Singh, S., Gupta, M.K., Nimdeo, Y.M., Raushan, R., Deorankar, A.V., Kumar, T.A., Rout, P.K., Chanotiya, C.S., Pakhale, V.D. and Nannaware, A.D., 2023. Solar energy: A promising renewable source for meeting energy demand in Indian agriculture applications. Sustainable Energy Technologies and Assessments, 55, p.102905. https://doi.org/10.1016/j.seta.2022.102905

Kusumawati, N., Setiarso, P., Santoso, A.B., Muslim, S., A'yun, Q., Putri, M.M., 2023. Characterization of poly (vinylidene Fluoride) Nanofiber-based electrolyte and its application to dye-sensitized solar cell with natural dyes. Indones J Chem 23, 113. https://doi.org/10.22146/ijc.75357

Lee, D.-K., Park, N.-G., 2022. Materials and methods for high-efficiency perovskite solar modules. Solar RRL 6. https://doi.org/10.1002/solr.202100455

Mahalingam, S., Manap, A., Rabeya, R., Lau, K.S., Chia, C.H., Abdullah, H., Amin, N., Chelvanathan, P., 2023. Electron transport of chemically treated graphene quantum dots-based dye-sensitized solar cells. Electrochimica Acta 439, 141667. https://doi.org/10.1016/j.electacta.2022.141667

Meng, L., Li, L., 2022. Recent research progress on operational stability of metal oxide/sulphide photoanodes in photoelectrochemical cells. Nano Research Energy. 1.2.

Moharam, M.M., El Shazly, A.N., Anand, K.V., Rayan, D.E.A., Mohammed, M.K.A., Rashad, M.M., Shalan, A.E., 2021. Semiconductors as effective electrodes for dye sensitized solar cell applications. Top Curr Chem (Cham) 379, 20. https://doi.org/10.1007/s41061-021-00334-w

Nadia, S.R., Khanmirzaei, M.H., Ramesh, S., Ramesh, K., 2017. Quasi-solid-state agar-based polymer electrolytes for dye-sensitized solar cell applications using imidazolium-based ionic liquid. Ionics 23, 1585-1590. https://doi.org/10.1007/s11581-016-1946-0

Nastasi, B., Markovska, N., Puksec, T., Duić, N. and Foley, A., 2022. Renewable and sustainable energy challenges to face for the achievement of Sustainable Development Goals. Renewable and Sustainable Energy Reviews, 157, p.112071. https://doi.org/10.1016/j.rser.2022.112071

Østergaard, P.A., Duic, N., Noorollahi, Y. and Kalogirou, S., 2022. Renewable energy for sustainable development. Renewable energy, 199, pp.1145-1152. https://doi.org/10.1016/j.renene.2022.09.065

Pirdaus, N.A., Nordin Amini, I.N., Imad Wan Mohtar, W.A.A.Q., Shamil Abd Aziz, M.A., Ahmad, N., 2023. Effect of deposition layer of titanium dioxide (TIO2) thin film as photoanode for economically sustainable dye-sensitized solar cell (DSSC) application. IJAREMS 12. https://doi.org/10.6007/ijarems/v12-i3/19238

Prabakaran, K., Jandas, P.J., Mohanty, S., Nayak, S.K., 2018. Synthesis, characterization of reduced graphene oxide nanosheets and its reinforcement effect on polymer electrolyte for dye sensitized solar cell applications. Solar Energy 170, 442-453. https://doi.org/10.1016/j.solener.2018.05.008

Sampaio, P.G.çalvesV., González, M.O.A., 2022. A review on organic photovoltaic cell. Intl J of Energy Research 46, 17813-17828. https://doi.org/10.1002/er.8456

Sasikumar, R., Thirumalaisamy, S., Kim, B., Hwang, B., 2024. Dye-sensitized solar cells: Insights and research divergence towards alternatives. Renew Sustain Energy Rev 199, 114549. https://doi.org/10.1016/j.rser.2024.114549

Saud, P.S., Bist, A., Kim, A.A., Yousef, A., Abutaleb, A., Park, M., Park, S.-J., Pant, B., 2024. Dye-sensitized solar cells: Fundamentals, recent progress, and optoelectrical properties improvement strategies. Optical Materials 150, 115242. https://doi.org/10.1016/j.optmat.2024.115242

Sayed, E.T., Olabi, A.G., Alami, A.H., Radwan, A., Mdallal, A., Rezk, A. and Abdelkareem, M.A., 2023. Renewable energy and energy storage systems. Energies, 16(3), p.1415. https://doi.org/10.3390/en16031415

Senthil, R.A., Theerthagiri, J., Madhavan, J., Ganesan, S., Arof, A.K., 2017. Influence of organic additive to PVDF-HFP mixed iodide electrolytes on the photovoltaic performance of dye-sensitized solar cells. J Phys Chem Solids 101, 18-24. https://doi.org/10.1016/j.jpcs.2016.10.007

Singh, R., Bhattacharya, B., Gupta, M., Rahul, Khan, Z.H., Tomar, S.K., Singh, V., Singh, P.K., 2017. Electrical and structural properties of ionic liquid doped polymer gel electrolyte for dual energy storage devices. Int J Hydrogen Energy 42, 14602-14607. https://doi.org/10.1016/j.ijhydene.2017.04.126

Solak, E.K., Irmak, E., 2023. Advances in organic photovoltaic cells: A comprehensive review of materials, technologies, and performance. RSC Adv. 13, 12244-12269. https://doi.org/10.1039/d3ra01454a

Starzak, K., Tomal, W., Chachaj-Brekiesz, A., Galek, M., Ortyl, J., 2024. Revealing the photoredox potential of azulene derivatives as panchromatic photoinitiators in various light-initiated polymerization processes. Polym Chem 15, 2931-2948. https://doi.org/10.1039/d4py00275j

Su'ait, M.S., Rayung, M., Ibrahim, S. and Ahmad, A., 2023. Bio-Based Polyurethane Polymer Electrolyte for Dye Solar Cells Application. In Polyurethanes: Preparation, Properties, and Applications Volume 3: Emerging Applications (pp. 37-62). American Chemical Society. doi: 10.1021/bk-2023-1454.ch002

Sundaramoorthy, K., Muthu, S.P., Perumalsamy, R., 2020. Effects of 2-Amino-4,6-Dimethoxypyrimidine \ton PVDF/KI/I2-Based Solid Polymer Electrolytes for dye-sensitized solar cell application. Journal of Elec Materi 49, 3728-3734. https://doi.org/10.1007/s11664-020-08070-5

Venkatesan, S., My, N.H.T., Teng, H., Lee, Y.-L., 2023. Thin films of solid-state polymer electrolytes for dye-sensitized solar cells. J Power Sources564, 232896. https://doi.org/10.1016/j.jpowsour.2023.232896

Wang, T., Yu, Q., Li, Z., Gao, Y., Huang, H., Dong, C., Yang, C., Chong, S., Wang, W. and Zhang, J., 2025. The potential of solid-state potassium-ion batteries with polymer-based electrolytes. Carbon Energy, p.e670. https://doi.org/10.1002/cey2.670

Wang, X., Zhang, Y., Xu, Q., Xu, J., Wu, B., Gong, M., Xiong. S., 2015. A low-cost quasi-solid DSSC assembled with PVDF-based gel electrolyte plasticized by PC–EC electrodeposited Pt counter electrode. J Photochem Photobiol A: Chem, 311, 112-117.

Zakaria, Z., Kamarudin, S.K., Osman, S.H., Mohamad, A.A., Razali, H., 2023. A review of carrageenan as a polymer electrolyte in energy resource applications. J Polym Environ 31, 4127-4142. https://doi.org/10.1007/s10924-023-02903-0

Zakiyah, N., Kusumawati, N., Setiarso, P., Muslim, S., A'yun, Q., Putri, M.M., 2024. Characterization and application of natural photosensitizer and poly (vinylidene Fluoride) nanofiber membranes-based electrolytes in DSSC. Indones J Chem 24, 701. https://doi.org/10.22146/ijc.86386

Zhou, J., Huang, Q., Ding, Y., Hou, G., Zhao, Y., 2022. Passivating contacts for high-efficiency silicon-based solar cells: From single-junction to tandem architecture. Nano Energy 92, 106712. https://doi.org/10.1016/j.nanoen.2021.106712